

Chemically Synthesised $Cd_{1-x}Zn_xSe$ thin films: Spectro-structural and microscopic studies

D. S. SUTRAVE, G. S. SHAHANE

*D.B.F. Dayanad College of Arts and Science,
413002, M S Solapur-INDIA*

V. B. PATIL, L. P. DESHMUKH

*Thin Film and Solar Studies Research Group,
Department of Physics (Appl. Electronics) and
Electronic Sciences, Shivaji University Centre
for P.G. Studies, Old Medical Colloge,
413003, M S Solapur-INDIA*

Received 17.06.1999

Abstract

This paper presents information pertaining to the chemo-mechanical synthesis of (Cd,Zn) Se thin films with a variable composition which has been brought about with the objective to study deposition history and growth kinetics, as well as structural changes and the optical properties. The effect of various process parameters, such as deposition time and temperature, concentration of species, speed of the substrate rotation, pH etc., on the growth and quality of the films is studied experimentally. At first sight, mechanistic interpretation of the reaction mechanism is given based on the influence of the process parameters on the film growth and the compositional, structural, microscopic and optical characteristics of $Cd_{1-x}Zn_xSe$ thin films. The films are crystalline over the whole range studied with a predominant wurtzite structure for $0 \leq x < 0.2$ and a zinc blende structure (solid solution) for $0.7 < x \leq 1$. The film compositions in the middle of the range ($0.2 \leq x < 0.7$) include both the cubic and the hexagonal structures. The crystal size determined from XRD and SEM micrographs, is observed to decrease with increasing x (up to $x=0.5$). The optical gap determination showed a non linear increase in the band gap with increasing Zn content in the film.

1. Introduction

Pseudo binaries of II-VI, IV-VI and III-V group compounds are attracting a great deal of attention because of their potential abilities in a wide spectrum of optoelectronic devices

[1-12]. $Cd_{1-x}Zn_xSe$ is one such promising ternary material for use in electroluminescent, photoluminescent, photoconductive and photovoltaic device applications [2,7-10,13,14]. It is a highly stable and resistive material with a band gap of about 2.0 eV (at $x=0.6$) [8, 13, 15], a band gap that nearly matches the maximum span of the visible region of the electromagnetic spectrum. The band structures, optical properties and crystal structures of both CdSe and ZnSe are very similar and therefore the system $Cd_{1-x}Zn_xSe$ not only can feasibly have a graded energy gap of a broad spectral sensitivity but many more material characteristics can perhaps be altered and very well controlled via system composition x . Both CdSe and ZnSe are known to exist in either cubic zinc blende or hexagonal wurtzite crystal forms, depending on the composition and the conditions of the preparation [8-10,13,14,16]. Thin films of these materials have been synthesised mainly via vacuum techniques. However, we have already established that growth by solution bath technique is extremely simple and viable compared to the other cost intensive methods [5,6,17]. Especially, one of the attractive features of the chemosynthesis approach is the ease with which the alloys can be generated without the use of any sophisticated instrumentation and process control. Therefore, we have investigated the synthesis of (Cd,Zn)Se thin films by our well defined chemical deposition process and report on some of the film properties with a special emphasis given to the deposition process and film composition.

2. Experimental Details

2.1 Synthesis of the $Cd_{1-x}Zn_xSe$ thin films

$Cd_{1-x}Zn_xSe$ samples were synthesised onto glass substrates from an alkaline bath consisting of Cd^{2+} , Zn^{2+} and Se^{2-} ions present simultaneously. The composition parameter x was obtained by adjusting the volume concentrations of Cd^{2+} and Zn^{2+} ions in the reaction container. For this, equimolar solutions of the cadmium sulphate and zinc sulphate in appropriate volume were complexed together by means of a triethanolamine and ammonia. The chalcogen ions (Se^{2-}) were provided to the system externally. They were added at a constant rate by adding sodium selenosulphate in the reaction bath. The reaction was allowed to take place for 3 hours at a pH value around 10 ± 0.2 . Sodium hydroxide solution was used to control the pH value. Clean microslide glasses of the suitable dimension were mounted on a specially designed substrate holder and were kept rotating at 70 ± 2 rpm speed in the reaction bath. The deposition temperature was maintained at $70\pm 2^\circ C$.

2.2 Techniques of characterisation

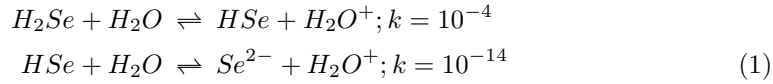
The layer thickness of the various samples was determined by an interference technique. XRD traces of the as grown films were recorded (Philips PW - 1710) for $2\theta = 10^\circ - 80^\circ$ with $CuK_\alpha(1.54060\text{\AA})$ radiation. The optical absorption spectra were obtained in the 300-900 nm wavelength range by employing a Spectronic- 20D spectrophotometer.

A 250 MK III stereoscan (USA) scanning electron microscope was used for the microscopic observations. Compositional analysis was carried out with an Atomic Absorption Spectrophotometer [Perkins Elmers 330(USA)].

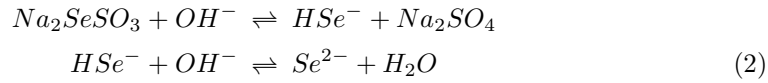
3. Results and Discussion

3.1 Kinetic studies

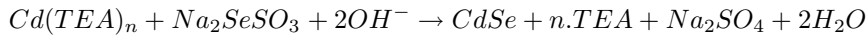
The decomposition of sodium selenosulphate is made possible in an aqueous alkaline medium containing the cadmium and zinc sulphate and a triethanolamine (TEA) complexing agent that allows us to control the Cd^{2+} , Zn^{2+} ion concentrations and to have a soluble species of Cd^{2+} and Zn^{2+} in the reaction bath. The deposition process is based on the slow release of Cd^{2+} , Zn^{2+} and Se^{2-} ions in solution which then condense, on an ion-by-ion basis, onto the substrates that are vertically mounted in the reaction solution. Due to the fact that the solubility products of metal selenides are very small and, in our case they are very similar [$K_{sp}(CdSe) \cong 10^{-33}$ and $K_{sp}ZnSe \cong 10^{-31}$], control of Cd^{2+} and Zn^{2+} ions in a reaction bath controls the rate of precipitation and consequently the rate of deposition. It is possible to obtain hydrolysis equilibrium and the H_2Se dissociation equilibrium due to the selenide ions [16]:



The above reaction sequence shows that the dominant species in solution is the HSe^- ions and Se^{2-} ions concentration is low. However, it could be increased by the addition of excess hydroxide ions according to



Of course, there are several possible soluble and insoluble species of Cd^{2+} and Zn^{2+} in a reaction bath containing OH^- . In our case the deposition was carried out on the thoroughly cleaned and ultrasonically dried commercial glass strips. The deposition solutions were prepared using analytical grade reagents and the glass strips were mounted vertically in a reaction container (consisting of Cd^{2+} and Zn^{2+} complex ions) such that more than two third portion of the glass strips was immersed in the solution. Se^{2-} ions were provided externally to the system at a constant rate when an appropriate temperature was reached and maintained by a temperature controlled oil bath. In an aqueous bath both Cd^{2+} and Zn^{2+} ions present the following global equilibrium reactions;



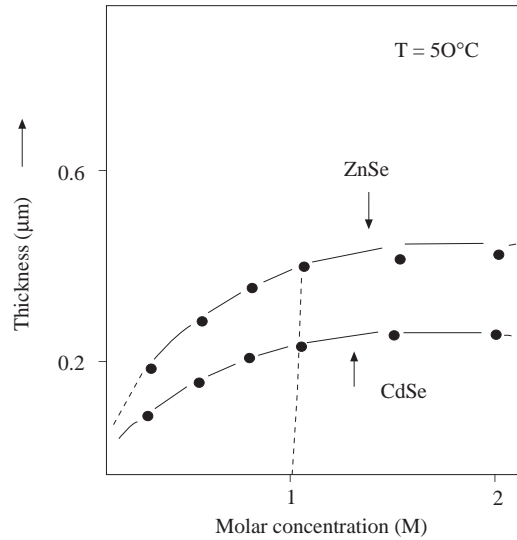
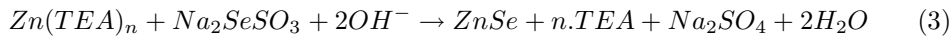


Figure 1. Variation of film thickness with concentration of Cd^{2+} and Zn^{2+} species ($T=50^\circ\text{C}$).

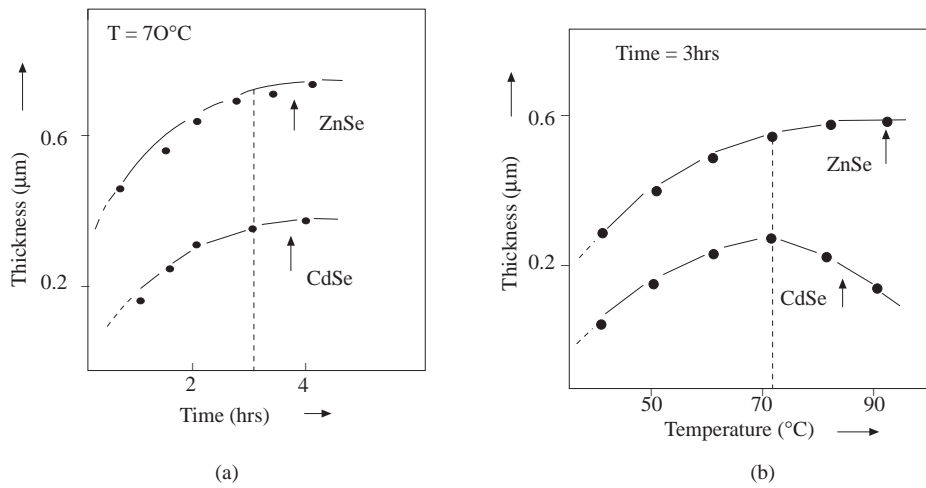


Figure 2. Film growth studies as a function of; a) Time and b) Temperature (at optimum concentration)

From the view point of kinetic studies, it appears from the above reactions that an increase of growth rate is expected when the concentrations of the basic ingredients in the bath are increased. Experimentally we have observed that growth rate initially is almost linear with the molar concentration [Fig. 1] and then saturates for further increase in

the concentration of the species in the bath. The optimum values of the concentrations of Cd^{2+} and Zn^{2+} ions were kept constant throughout the experiment and are 1M. The second important aspect in our physical studies is the influence of the deposition time and temperature on film formation. The film growth on glass strip surface has been studied as a function of both temperature and the deposition time (Fig. 2a,b). It can be seen that the deposition mechanism clearly shows two different growth stages; an initial quasilinear and a saturation. The initial growth rate can be calculated only in the quasilinear stage. The second stage is characterised by means of a saturation phenomena which seems to be mainly due to the depletion of Cd^{2+} , Zn^{2+} and Se^{2-} species in the reaction bath. At higher temperature this saturation stage appears earlier and is due to the two competitive processes; the film formation and the homogeneous precipitation as explained earlier by us [18] and Dona and Herrero [16]. An increase in the deposition temperature favours the homogeneous precipitation rather than the film formation which causes saturation to occur. The best conditions in the deposition process for yielding good quality deposits are 70°C and 3 hours, respectively.

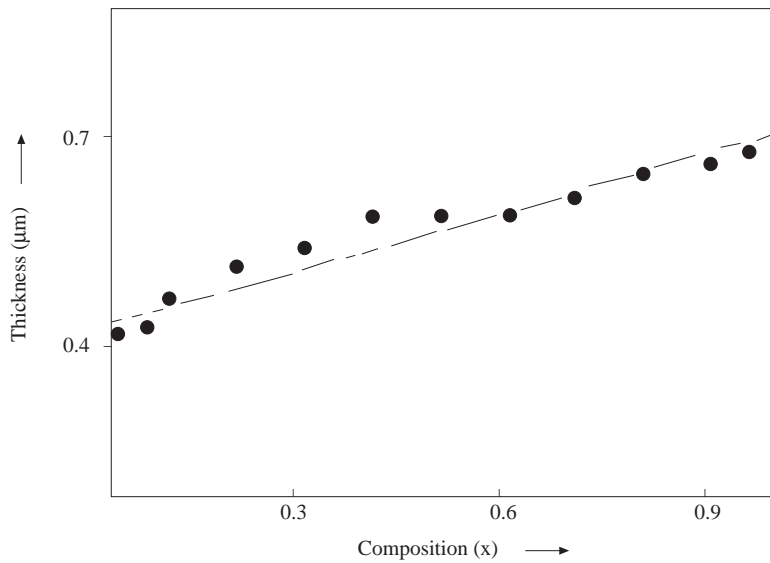


Figure 3. Dependence of film thickness on composition parameter, x .

As one of the physical parameters, the effect of film composition (x) on the film thickness was also studied and is found to increase almost linearly with x (Fig. 3) as expected. The $Cd_{1-x}Zn_xSe$ film layers obtained by this technique were diffusely reflecting and adhered tightly to the substrate surface. The as-grown CdSe samples were dark orange-red in color whereas pure ZnSe exhibited white color with a slight greyish tinge. The color of the $Cd_{1-x}Zn_xSe$ deposits changed from an orange-red to greyish white as x was varied from 0 to 1.

The $Cd_{1-x}Zn_xSe$ films were then analysed compositionally by an atomic absorption spectroscopy technique. The results show that x_{film} parameter for the film is not equal to that with x_{bath} ; their relation being non linear (Fig.4).

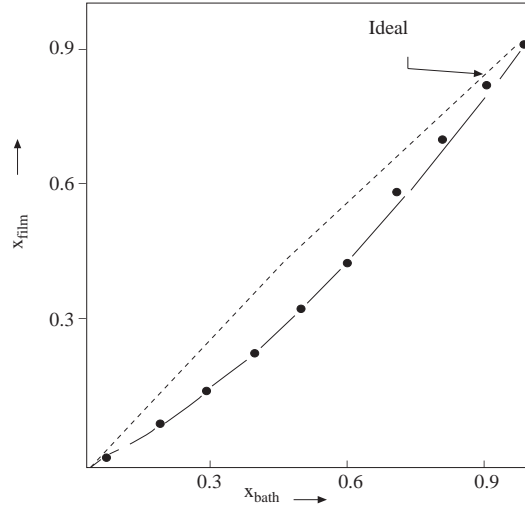


Figure 4. Compositional analysis : x_{bath} vs. x_{film}

Structural studies

The crystal structure has been determined within the 2θ range of $10^\circ - 80^\circ$ by X-ray diffraction analysis for samples in the composition range $0 \leq x \leq 1$ (Fig. 5). It is seen that all the samples are crystalline over the whole range studied. Table 1 summarises the results of the various crystallographic phases and their intensities of reflections for a few of the hkl planes. It appears from the Table 1 that pure CdSe exhibits both hexagonal wurtzite (dominant) and cubic zinc blende structures, whereas ZnSe is only structurally cubic. The analysis showed that Zn has three important roles depending upon the concentration, when incorporated into the lattice of CdSe. For the range $0 < x \leq 0.2$ it has a strong tendency of replacing Cd from the lattice with a corresponding decrease in the peak (101, hex) intensity without any appreciable shifting (Fig.6).

For $0.2 < x \leq 0.7$ range, intensity remained more or less constant (up to $x \leq 0.5$) and the number of peaks of both hexagonal and cubic CdSe phases have been found to be little increased, whereas the cubic ZnSe phase continuously increased showing that the $Cd_{1-x}Zn_xSe$ films are the admixture of the CdSe and ZnSe phases in this range. For these ranges, cubic ZnSe did not form a solid solution with either of the phases. Only a Zn substitution effect was observed. This is further supported by the smaller interplanar distances for $0 \leq x \leq 0.2$ [19] and formation of the separate phases in the $0.2 < x \leq 0.7$ range. Of course, possibility of negligibly small amount of solid solution in these regions can not be ruled out.

Table 1. The description of the crystallographic structures (phases) of $Cd_{1-x}Zn_xSe$ thin films.

Composition range	CdSe		ZnSe		Observations
	Cubic	Hexagonal	Cubic	Intensity	
CdSe	phase	phase	phase	peak	
	√	√	-	-	-
$0 < x \leq 0.2$	mod	max	max	max	-
	√	√	-	-	-
$0.2 < x \leq 0.5$	I	I	I	I	C(min)
	min	-	-	-	-
$0.5 < x \leq 0.7$	I	C	C	I	C
	min	-	-	-	-
$0.7 < x \leq 1$	C	D	D	I	I
	√	min	-	-	-
ZnSe	min	-	-	-	-
	√*	√	√	√	I
	√	√	√	√	-
	-	-	-	max	max
	-	-	-	-	-
	-	-	√	√	-
	-	-	-	-	-
	-	-	√	√	-

√ = presence of phases, min=minimum, mod=moderate, max=maximum, I=increases, D=decreases, C=constant. First line represent our findings and the second line is report of other workers.

* In addition to the solid solution few peaks of cubic CdSe have also been found.

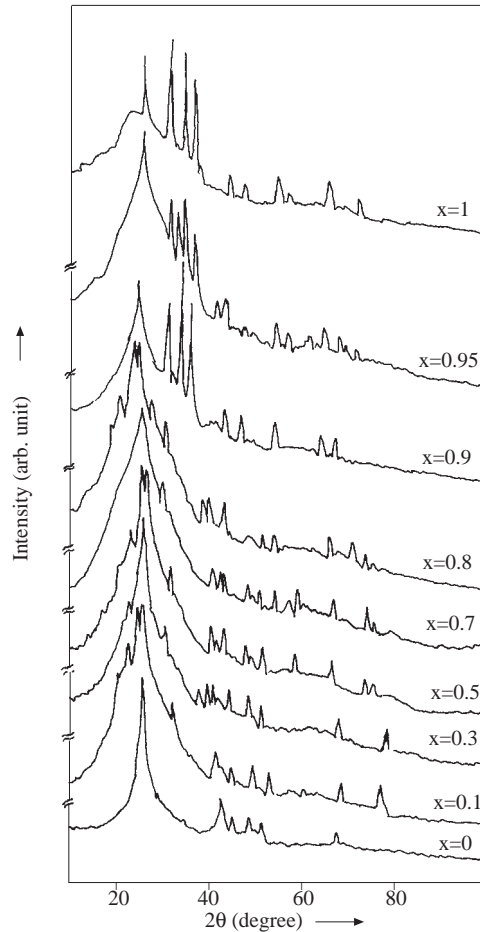


Figure 5. X-ray diffractogram traces of nine typical films with various x values (on glass substrates)

For zinc dominated films ($0.7 < x \leq 1$), Cd shifts the peak (111 cubic) position continuously towards lower 2θ values showing the solid solution formation in this region. Similarly, other peaks of cubic ZnSe (200), (220), (222), (331), (400), and (420) are also found to be shifted towards higher d -values. A peak corresponding to (200) reflection of ZnSe ($d = 2.837 \text{ \AA}$) seems to be through out the x values (except at $x=0$).

On the ZnSe side the intensity is maximum, where as it is more or less constant on the CdSe side. The variation in lattice parameter has also been examined (Fig. 7) in the solid solution region. It is found that the lattice parameter a changed typically from 5.681 \AA to 5.776 \AA for the change of x from 1 to 0.7. It is notable for this range that the peaks corresponding to hexagonal CdSe are totally absent. The average crystallite size was determined for all the compositions and are listed in Table 2.

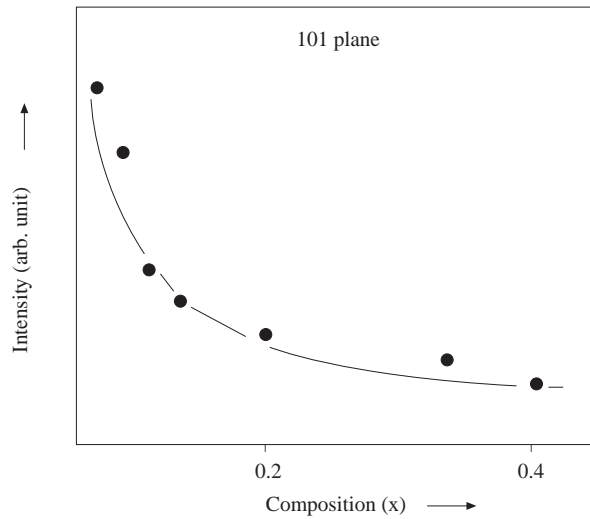


Figure 6. Variation of intensity of (101) reflection of hexagonal CdSe with x

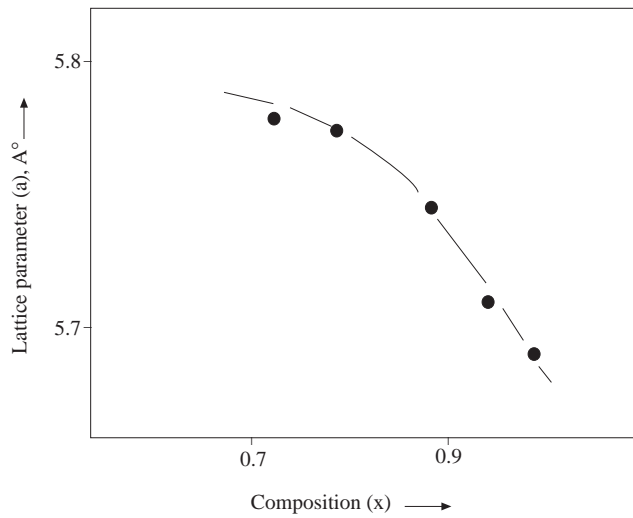


Figure 7. Variation of lattice parameter a with composition x

3.3 Microscopic observations

The $Cd_{1-x}Zn_xSe$ films were examined in a scanning electron microscope (Fig. 8). The polycrystalline texture with a rough surface and clearly defined grains has been observed for all the samples. As-deposited CdSe appears crystalline and is composed of big grains overgrown on uniformly distributed spherical smaller grains of poorly defined edges embedded in it. It can be stated in this case that nucleation of fresh CdSe

molecules occurs over the already grown CdSe molecules during the deposition process. The resulting picture looks like a cauliflower-like growth over a background of uniformly distributed smaller grains and that the smaller grains fill up the gaps in big cauliflower type grains. The films grow in both hexagonal wurtzite and cubic zinc blende forms; the hexagonal phase being dominant (see section 3.2). The hexagonal structure appears needle-like microcrystals of larger size whereas spherical grains significantly smaller in size are that of the cubic phase. These hexagonal microcrystals grow at the expense of cubic microcrystals [24] showing either the cauliflower or leafy cabbage type mixed structures.

The SEM micrograph of a continuous pure ZnSe film (Fig.8j) shows a globular structure of clusters composed of a single type of small spherical densely packed microcrystals. The average crystallite size is determined for these samples and listed in Table 2. The observed discrepancy in the measurement of the grain size by XRD and SEM would be due to that the two or more crystallites may be fused/united together to form a particle obviously showing greater size. This is clearly seen for samples with $x > 0.5$. When Zn is incorporated into the lattice of CdSe, the samples still consist of more or less the same microstructure with an increased number of smaller grains reduced in size. This is true up to $x=0.5$ and is also supported by the XRD studies wherein a more or less constant amount of both hexagonal and cubic phases of CdSe with an increased ZnSe phase have been observed. For other compositions ($0.7 < x \leq 0.95$) it is surprising that the structure appears uniphase but altogether different showing the strong possibility of an alloy formation of CdSe and ZnSe as detected from the XRD studies. The grains become elongated, shapeless and much larger in size. It is very difficult to determine the crystal size in these cases from the SEM studies.

3.4 Optical studies

The optical absorption spectra of various $Cd_{1-x}Zn_xSe$ thin films corrected for glass substrate absorption were obtained and shown in Fig. 9. The spectra clearly indicated two regions; one for high wavelengths with practically negligible absorption and other for low wavelengths in which absorption increases steeply to a maximum value with a shift of absorption edge from 700 nm to 480 for the film composition modulation from 0 to 1. The variation of an energy gap (E_g) with the composition was determined from these optical adsorption experiments at room temperature. The measurements were used to obtain estimates for E_g from the position of the absorption edge. Plots of $(\alpha hv)^2$ vs hv for six typical compositions are shown in Fig. 10. The results show that the band gap varies smoothly and monotonically but not linearly over the composition range (Fig. 11). The dependence of the band gap on composition is often described by an empirical relation [9],

$$E_g(x) = E_g(CdSe) + [E_g(ZnSe) - E_g(CdSe) - b].x + bx^2, \quad (4)$$

where, b is known as the bowing parameter and x is the film composition. It appears from Fig 11 that for Cd-rich compositions ($x \ll 1$) E_g varies slowly with x whereas it is faster at the ZnSe end of the E_g spectrum. Such overestimation of quadratic dependence of band

gap for Zn-rich $Cd_{1-x}Zn_xSe$ films has already been reported [9,10]. Our observations for chemically deposited $Cd_{1-x}Zn_xSe$ films are in good agreement. The plots of $(\alpha hv)^2$ vs hv are linear in the high energy region indicating direct type of transitions in these films. The type of transitions was also determined by considering the relation between the absorption coefficient (α) and the photon energy (hv). They are related as:

$$\alpha = (A/h\nu)(hv - E_g)^m, \quad (5)$$

where, A is a constant and m is the power factor and assumes values 0.5, 2, 1.5 and 3 for allowed direct, allowed indirect, forbidden direct and forbidden indirect transitions, respectively [25].

For allowed direct transitions,

$$\alpha hv = A(hv - E_g)^{0.5} \quad (6)$$

and rearrangement yields

$$\ln(\alpha hv) = \ln(A) + 0.5\ln(hv - E_g). \quad (7)$$

Thus the plot of $\ln(\alpha hv)$ vs $\ln(hv - E_g)$ should yield a straight line whose slope gives the value of power factor (m) equal to 0.5. In our case, m values for all composite structures are determined and indicated in Table 2.

Table 2. Some of the characterisitic parameters of the (Cd, Zn) Se thin film structures.

Sr.No.	Composition parameter, x	Grain size (\AA°)		Power factor m
		From XRD	From SEM	
1	0.000	1157	5000	0.60
2	0.025	1134	-	0.50
3	0.050	1102	4100	0.46
4	0.075	1092	-	0.42
5	0.1	1080	3300	0.44
6	0.2	1160	-	0.42
7	0.3	1199	5200	0.50
8	0.4	1201	-	0.56
9	0.5	1129	4400	0.42
10	0.6	1201	5700	0.50
11	0.7	1192	-	0.48
12	0.8	1190	-	0.50
13	0.9	1201	-	0.48
14	0.95	1167	-	0.48
15	1.0	1167	5500	0.50

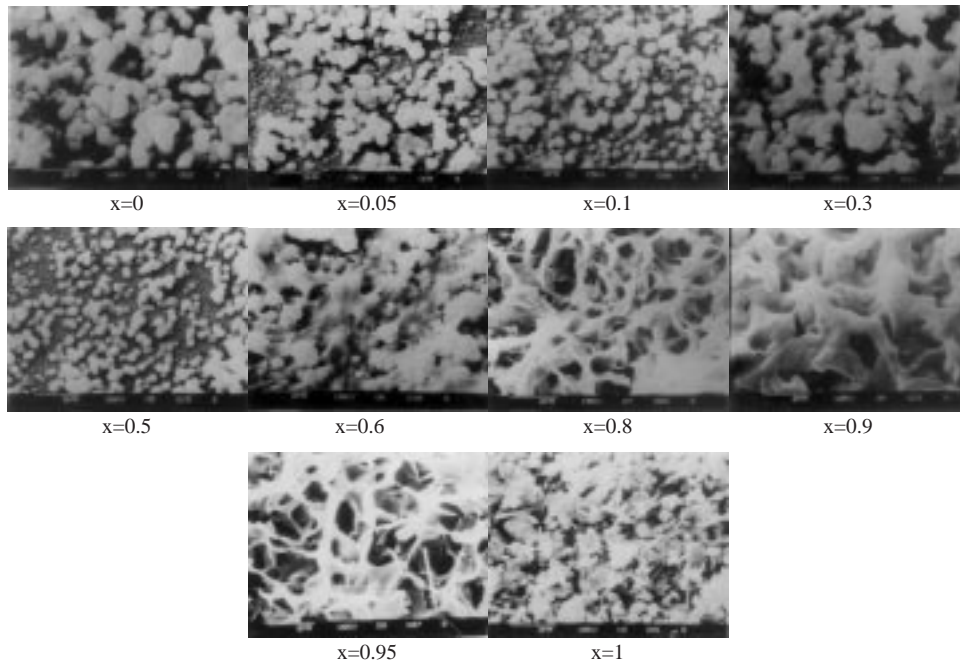


Figure 8. SEM micrographs of ten $Cd_{1-x}Zn_xSe$ films with various x -values (on glass substrates)

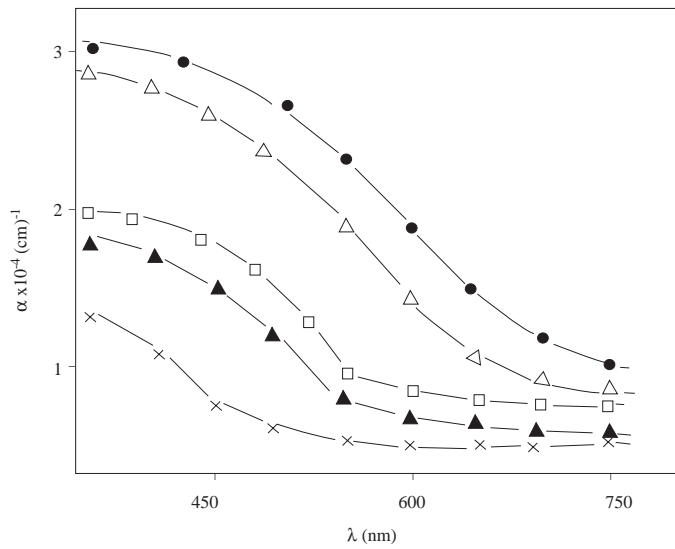


Figure 9. The optical absorption spectra of five typical (Cd, Zn) Se compositions. $\bullet \rightarrow x = 0$, $\square \rightarrow x = 0.2$, $\Delta \rightarrow x = 0.3$, $\blacktriangle \rightarrow x = 0.7$, $\times \rightarrow x = 1$

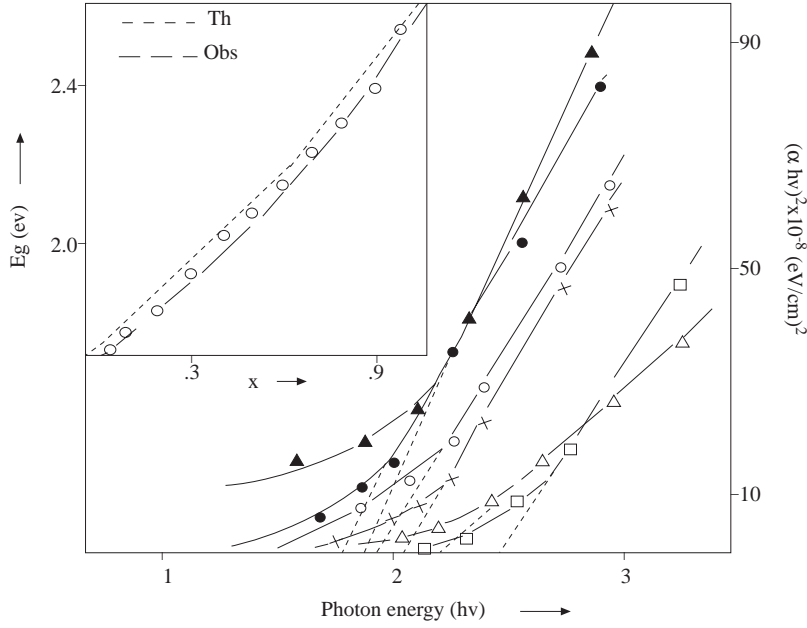


Figure 10. Variation of $(\alpha hv)^2$ vs hv for six representative $Cd_{1-x}Zn_xSe$ samples. $\bullet \rightarrow x = 0$, $\blacktriangle \rightarrow x = 0.1$, $\circ \rightarrow x = 0.2$, $\times \rightarrow x = 0.3$, $\Delta \rightarrow x = 0.4$, $\square \rightarrow x = 0.9$

4. Conclusions

We should like to note that the physical, structural and optical characteristic features observed for chemical bath synthesised $Cd_{1-x}Zn_xSe$ thin films have close agreement with what had been observed for other semiconductor solid solution systems which show their common characters. We have also shown that the alternations in the deposition history and chemical constituents in the (Cd, Zn) Se system lead to the composition scenarios ranging from a physical admixture of CdSe and ZnSe to a $Cd_{1-x}Zn_xSe$ solid solution and even the superstructures with approximately alternating stacks of CdSe and ZnSe layers can be built. These characteristics make the chemical bath process a simple, an inexpensive and attractive means of obtaining (Cd, Zn) Se thin films for a variety of applications.

References

- [1] N. C. Sharma, D. K. Pandya, H. K. Sehgal and K. L. Chopra, *Thin Solid Films*, 59, 157 (1979).
- [2] T. M. Razykov, *Thin Solid Films*, 164, 301 (1998).
- [3] A. K. Sood, K. Wu and J. N. Zemel, *Thin Solid Films*, 48, 73 (1978) and 48, 87 (1978).

- [4] J. A. Rodriguez and G. Gordillo, *Solar Energy Mater.*, 19, 421 (1989).
- [5] L. P. Deshmukh, K. M. Garadkar and D. S. Sutrave, *Mater. Chem. Phys.*, 55, 30(1998).
- [6] L. P. Deshmukh, B. M. More and S. G. Holikatti *Bull. Mater. Sci.*, 17, 455 (1994).
- [7] A. S. Nasibov, Y. V. Korostelin, L. G. Suslina, D. L. Fedorov and L. S. Markov, *Solid State Commun.*, 71, 867 (1989).
- [8] A. Burger and M. Roth, *J. Cryst. Growth* 70, 386 (1984).
- [9] A. A. Bassam, A. W. Brinkman, G. J. Russell and J. Woods, *J. Cryst. Growth*, 86, 667 (1998).
- [10] P. Gupta, B. Maity, A. B. Maity, S. Chaudhuri and A. K. Pal, *Thin Solid Films*, 260, 75 (1995).
- [11] J. M. Dona and J. Herrero, *Thin Solid Films*, 268, 5 (1995).
- [12] G. K. Padam, G. L. Malhotra and S. U. Rao, *J. Appl. Phys.*, 63, 770 (1988).
- [13] V. Krishna, D. Ham, K. K. Mishra and K. Rajeshwar, *J. Electrochem Soc.*, 139, 23 (1992).
- [14] N. Samarth, H. Leo, J. K. Furdyan, R. G. Alonso, Y. R. Lee, A. K. Ramdas, S. B. Quadri and N. Otsuka, *Appl. Phys. Lett*; 56, 1163 (1990).
- [15] K. C. Sharma and J. C. Garg, *Ind. J. Pure & Appl. Phys.*, 26, 480 (1988).
- [16] J. M. Dona and J. Herrero, *J. Electrochem. Soc.*, 142, 764 (1995).
- [17] L. P. Deshmukh, S. G. Holikatti and P. P. Hankare, *J. Phys. D: Appl. Phys.* 27, 1786 (1994).
- [18] L. P. Deshmukh, B. M. More, C. B. Rotti and G. S. Shahane, *Mater. Chem. Phys.*, 45, 145 (1996).
- [19] A. Darkowski and A. Grabowski, *Solar Energy Mater.*, 23, 175 (1991).
- [20] Xu-Rui. Xiao and H. T. Tien, *J. Electrochem Soc.*, 130, 55 (1983).
- [21] S. Chen, M. A. Russak, H. Witzke, J. Reichman and S. K. Deb, U. S. Patent No. 4172925 (1979).
- [22] G. Hodes, in : *Energy Resources Through Photochemistry and Catalysis*, (Ed.) M. Gratzel (Academic Press, New York 1983) Ch. 13.
- [23] Joint Committee on Powder Diffraction Standards (JCPDS No. 5-0522).
- [24] S. Bhushan and S. Shrivastav, *Ind. J. Pure & Applied Phys.* 33, 371 (1995).
- [25] D. Bhattacharya, S. Choudhuri and A. K. Pal, *Vacuum* 43, 313 (1992).